

Raman scattering by the E_{2h} and A₁(LO) phonons of In_xGa_{1-x}N epilayers (0.25 < x < 0.75) grown by molecular beam epitaxy

R. Oliva, J. Ibáñez, R. Cuscó, R. Kudrawiec, J. Serafinczuk et al.

Citation: *J. Appl. Phys.* **111**, 063502 (2012); doi: 10.1063/1.3693579

View online: <http://dx.doi.org/10.1063/1.3693579>

View Table of Contents: <http://jap.aip.org/resource/1/JAPIAU/v111/i6>

Published by the AIP Publishing LLC.

Additional information on J. Appl. Phys.

Journal Homepage: <http://jap.aip.org/>

Journal Information: http://jap.aip.org/about/about_the_journal

Top downloads: http://jap.aip.org/features/most_downloaded

Information for Authors: <http://jap.aip.org/authors>

ADVERTISEMENT



AIP Advances

Now Indexed in Thomson Reuters Databases

Explore AIP's open access journal:

- Rapid publication
- Article-level metrics
- Post-publication rating and commenting

Raman scattering by the E_{2h} and $A_1(\text{LO})$ phonons of $\text{In}_x\text{Ga}_{1-x}\text{N}$ epilayers ($0.25 < x < 0.75$) grown by molecular beam epitaxy

R. Oliva,¹ J. Ibáñez,¹ R. Cuscó,¹ R. Kudrawiec,² J. Serafinczuk,³ O. Martínez,⁴ J. Jiménez,⁴ M. Henini,⁵ C. Boney,⁶ A. Bensaoula,⁶ and L. Artús¹

¹*Institut Jaume Almera, Consell Superior d'Investigacions Científiques (CSIC), Lluís Solé i Sabarís s.n, 08028 Barcelona, Catalonia, Spain*

²*Institute of Physics, Wrocław University of Technology, Wybrzeże Wyspiańskiego 27, 50-370 Wrocław, Poland*

³*Faculty of Microsystem Electronics and Photonics, Wrocław University of Technology, Janiszewskiego 11/17, 50-372 Wrocław, Poland*

⁴*Departamento de Física de la Materia Condensada, Cristalografía, y Mineralogía, Universidad de Valladolid, 47011 Valladolid, Spain*

⁵*Nottingham Nanotechnology and Nanoscience Centre, University of Nottingham, Nottingham NG7 2RD, United Kingdom*

⁶*Department of Physics, University of Houston, 4800 Calhoun, Houston, Texas 77004, USA*

(Received 16 November 2011; accepted 14 February 2012; published online 16 March 2012)

We use Raman scattering to investigate the composition behavior of the E_{2h} and $A_1(\text{LO})$ phonons of $\text{In}_x\text{Ga}_{1-x}\text{N}$ and to evaluate the role of lateral compositional fluctuations and in-depth strain/composition gradients on the frequency of the $A_1(\text{LO})$ bands. For this purpose, we have performed visible and ultraviolet Raman measurements on a set of high-quality epilayers grown by molecular beam epitaxy with In contents over a wide composition range ($0.25 < x < 0.75$). While the as-measured $A_1(\text{LO})$ frequency values strongly deviate from the linear dispersion predicted by the modified random-element isodisplacement (MREI) model, we show that the strain-corrected $A_1(\text{LO})$ frequencies are qualitatively in good agreement with the expected linear dependence. In contrast, we find that the strain-corrected E_{2h} frequencies exhibit a bowing in relation to the linear behavior predicted by the MREI model. Such bowing should be taken into account to evaluate the composition or the strain state of InGa_N material from the E_{2h} peak frequencies. We show that in-depth strain/composition gradients and selective resonance excitation effects have a strong impact on the frequency of the $A_1(\text{LO})$ mode, making very difficult the use of this mode to evaluate the strain state or the composition of InGa_N material. © 2012 American Institute of Physics.

[<http://dx.doi.org/10.1063/1.3693579>]

I. INTRODUCTION

Group-III nitride semiconductors (AlN, GaN, InN, and related alloys) are already employed in a variety of commercial device applications, including InGa_N/GaN light emitting diodes and lasers operating in the green-to-blue spectral range, and AlGa_N/GaN high-power microwave transistors. The discovery of the low energy bandgap value of InN (0.67 eV) gave rise to renewed research interest in the InGa_N ternary alloy, the bandgap of which can be tuned to cover the entire visible spectral range, from the ultraviolet (UV) down to near-infrared wavelengths. This unique property could be exploited for the fabrication of high-efficiency multijunction solar cells, infrared detectors or white-light emitting devices. However, the performance of the applications based on In-rich InGa_N alloys is still limited by the poor crystalline quality of the as-grown material. A great deal of research work is currently being devoted to produce InGa_N samples with improved crystal quality.^{1,2}

Raman scattering is a highly valuable tool to investigate and characterize semiconductor materials and structures. In the case of ternary and quaternary alloys, Raman scattering provides a powerful, non-destructive means to evaluate the

composition of the samples (see Ref. 3 for a review on III-V alloys). Numerous studies have been devoted to study the vibrational properties of hexagonal InGa_N thin films^{4–21} and InGa_N/GaN quantum wells.^{22–24} Although it is well accepted that both the $A_1(\text{LO})$ and the E_{2h} phonon modes of InGa_N display a one-mode behavior,^{15,16} there are still open questions regarding the behavior of the optical phonons in the InGa_N alloy. While the modified random-element isodisplacement (MREI) model²⁵ predicts that the frequency of both modes varies linearly from those of the two binary end-members (GaN and InN), some authors have measured E_{2h} frequencies that seem to exhibit a significant bowing in relation to the linear frequency dependence.^{9,10,13,21} On the other hand, strong deviations from the linear behavior have also been observed for the $A_1(\text{LO})$ polar mode of bulk InGa_N (see for instance the data over the whole composition range reported in Ref. 16). Such deviations are usually attributed to the strain of the samples.^{12,20} However, many authors have shown that the $A_1(\text{LO})$ frequency strongly depends on the excitation wavelength and/or on temperature, and different effects have been invoked to explain the observations: i) strain and/or compositional gradients over depth,^{13,19} ii) compositional inhomogeneities giving rise to selective

resonant excitation of domains with a particular In content;^{5,7,15,17} iii) relaxation of the wave-vector selection rule.¹⁸ Thus, it remains necessary to identify which mechanisms are actually playing a key role in the behavior of the $A_1(\text{LO})$ mode of InGaN.

In the present work we use resonant and non-resonant Raman scattering to investigate the behavior of the $A_1(\text{LO})$ and E_{2h} modes in $\text{In}_x\text{Ga}_{1-x}\text{N}$ epilayers grown by molecular beam epitaxy (MBE) ($0.25 < x < 0.75$). Given that the frequency of the optical phonons is highly sensitive to the strain state and composition of the samples, we first present a structural and optical characterization of the InGaN epilayers. High-resolution x-ray diffraction (HRXRD) is used to determine the In composition and the strain state of the InGaN epilayers. The In content of the epilayers is further confirmed by photoluminescence (PL) and cathodoluminescence (CL) measurements. The degree of (lateral) compositional homogeneity of the samples is also studied by CL. Both the resonant and non-resonant spectra reveal that the frequency of the $A_1(\text{LO})$ mode strongly deviates from the expected linear dependence in the samples with $0.25 < x < 0.44$. We show that such strong deviations can be mainly attributed to strain effects. In contrast, we find that the strain-corrected E_{2h} frequencies are redshifted over the whole composition range in relation to the linear behavior, in agreement with previous observations on Ga-rich samples.^{9,10} The possible role of lateral compositional fluctuations and in-depth strain/composition gradients on the frequency behavior of the $A_1(\text{LO})$ mode of InGaN is analyzed and discussed.

II. EXPERIMENT

The InGaN epilayers used in this work, with nominal thicknesses in the 0.2–0.96 μm range, were grown by plasma-assisted MBE on (0001)-sapphire substrates with a 4- μm thick GaN buffer layer. Details of the growth procedure can be found elsewhere.²⁶ HRXRD measurements were performed with a Philips X-Pert PRO diffractometer. Reciprocal space maps (RSMs) around the symmetrical (00.2) and the asymmetrical (11.4) and (01.5) reflections were obtained. From the analysis of the RSMs, the composition and strain state of the InGaN epilayers were evaluated. For details of the procedure, see Ref. 27. Table I shows the In molar fraction and the degree of plastic relaxation of these samples as obtained from the RSMs.

TABLE I. Indium molar fraction (x), degree of plastic relaxation (R), and thickness (d) of the MBE-grown $\text{In}_x\text{Ga}_{1-x}\text{N}$ epilayers studied in this work. For samples A969, A1004, A1035, and A1177, x and R were obtained from HRXRD measurements. For samples A1018 and A1182, x and R were estimated by using the HRXRD data from similar InGaN epilayers.

Sample	In content (x)	Plastic relaxation (R) (%)	Thickness (d) (nm)
A969	0.25	68%	200
A1004	0.33	40%	960
A1010	0.34	57%	710
A1018	0.42	~50%	710
A1035	0.44	50%	560
A1177	0.68	100%	500
A1182	0.75	~100%	500

PL spectra were acquired with a FHR1000 Jobin-Yvon spectrometer equipped with a Peltier-cooled CCD camera (514.5-nm excitation). Sample A1182 ($x=0.75$) was not included in the PL study because the optical emission of this sample is below the detection limit of the experimental setup. CL measurements were performed in order to study the lateral homogeneity of the InGaN layers at the sub-micron scale. The CL measurements were carried out at low temperature (80 K) on four of the samples (A969, A1004, A1010, and A1018). A XiCLOne (Gatan UK) CL system equipped with a Peltier-cooled charge-coupled device (CCD) camera was employed.

Raman scattering measurements were performed at room temperature in backscattering configuration using a Jobin-Yvon T64000 spectrometer equipped with a liquid N_2 -cooled CCD. The experiments were carried out with the 514.5-nm line of an Ar^+ laser for resonant or near-resonant excitation conditions (samples with $0.25 \lesssim x \lesssim 0.44$), and with the 325.0-nm line of an He-Cd laser for non-resonant conditions.

III. RESULTS AND DISCUSSION

A. Structural and optical-emission characterization

Given that the frequency of the optical phonons of InGaN is strongly affected by the In content and strain state of the samples, we first carried out a structural and optical characterization of the InGaN epilayers studied in this work. HRXRD measurements were performed to evaluate the composition and the degree of lattice-constant relaxation in six of the samples (A969, A1004, A1010, A1035, and A1177). Figure 1 shows selected x-ray rocking curves [(00.2) reflection] for samples A1004 ($x=0.33$), A1035 ($x=0.44$), and A1177 ($x=0.68$). Importantly, no phase segregation is observed in any of the rocking curves. The broadening of the x-ray reflections suggests that strain and/or composition gradients may exist along the growth direction. Lateral composition/strain fluctuations may also contribute to the observed broadening.

The nominal thickness of all the InGaN epilayers studied here, in the 0.2–0.96 μm range, is above the expected critical layer thickness.²⁸ Thus, a partial strain relaxation can be anticipated in all the epilayers. RSMs around the symmetrical (00.2) and the asymmetrical (11.4) or (01.5) reflections

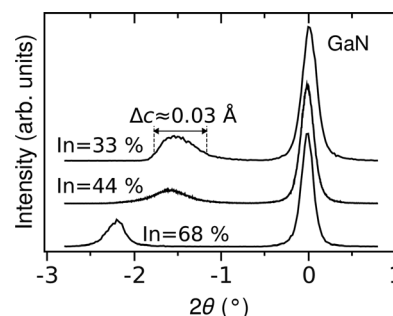


FIG. 1. HRXRD rocking curve corresponding to the (00.2) reflection of three $\text{In}_x\text{Ga}_{1-x}\text{N}$ epilayers with $x=0.33$ (sample A1004), $x=0.44$ (sample A1035), and $x=0.68$ (sample A1177).

were obtained for samples A969, A1004, A1010, A1035, and A1177 (not shown). From both the symmetrical and asymmetrical RSMs, information about the in-plane and out-of-plane lattice spacings can be simultaneously obtained, and thus the average In content and the strain state of the InGaN epilayers can be evaluated.²⁷ In the case of samples A1018 and A1182, the In composition and the degree of lattice relaxation have been evaluated by using the HRXRD data of InGaN epilayers grown under similar conditions. On the other hand, sample A969 exhibited a fairly nonuniform color across the whole wafer. Most probably, the results obtained for this particular sample have larger errors than those obtained for the rest of epilayers. Table I shows the In molar fraction and the degree of plastic relaxation, R , thus obtained. $R(\%)$ is defined as a function of the in-plane component of the strain tensor for the epilayer, $\epsilon_{\parallel} = [(a - a_0)/a_0]$ (a is obtained from the HRXRD measurements), so that $\epsilon_{\parallel} = -[(a_{\text{GaN}} - a_0)/a_0](R(\%) - 100)/100$, where a_{GaN} is the in-plane lattice parameter of the GaN substrate and $a_0 = xa_{\text{InN}} + (1 - x)a_{\text{GaN}}$ corresponds to the relaxed lattice parameter of $\text{In}_x\text{Ga}_{1-x}\text{N}$. As can be seen in Table I, the resulting R values show that only the In-rich samples ($x \gtrsim 0.68$) are fully relaxed, while the rest of samples are partially relaxed, with R values ranging from 40% to 70%.

As in the case of the HRXRD curves of Fig. 1, none of the RSMs obtained from our samples (not shown) displayed any signal of phase segregation. The RSMs confirmed that strain and/or composition gradients exist in these epilayers. However, the RSMs did not allow us to discern between composition and strain gradients, as performed for instance in Ref. 29. Nevertheless, the broadening of the x-ray peaks in Fig. 1 can still be used to obtain a rough estimation of the maximum variation of the lattice parameter along the growth direction, Δc , that may arise from in-depth strain and/or composition gradients. For this purpose, we use Bragg's law and assume that all the observed broadening in the (00.2) reflections is originated by in-depth changes in the lattice parameter c . Note that for the present discussion we are deliberately neglecting the contribution of other sources of peak broadening (i.e., the finite coherence length of the microcrystalline domains, microstrain effects, lateral compositional fluctuations, etc.) because our goal is to find an upper limit for the impact of in-depth compositional/strain gradients on the observed broadening. Thus, from the width of the (00.2) reflections we estimate that $\Delta c \lesssim 0.03$ Å in all our samples. In the following sections this value will be used to delimit the impact of strain and composition gradients on the frequency of the $A_1(\text{LO})$ phonon mode of InGaN.

To confirm the In-content values obtained by HRXRD and obtain additional information about the lateral homogeneity of the InGaN layers, PL and CL measurements were carried out on several of the samples studied in this work. The PL peak emission energy obtained for all the samples investigated (not shown) was found to be in good agreement with that measured on InGaN samples of similar compositions.³⁰ All samples displayed a single, well-defined PL emission band, thus confirming that no measurable phase segregation is present in our samples. This was further corroborated with CL measurements, which allow one to probe

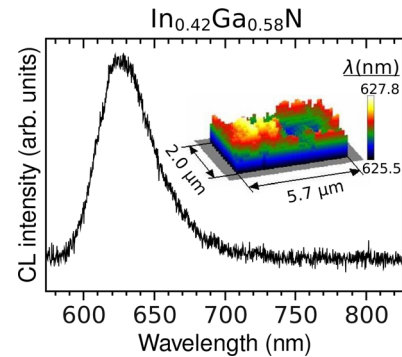


FIG. 2. (Color online) CL spectrum at 80 K of an $\text{In}_x\text{Ga}_{1-x}\text{N}$ epilayer with $x = 0.42$ (sample A1018). The inset shows a mapping of the CL peak wavelength over a sample region of $2 \mu\text{m} \times 6 \mu\text{m}$.

the compositional homogeneity of InGaN epilayers and heterostructures at the submicron scale.¹⁴ Fig. 2 shows a typical low-temperature (80 K) CL spectrum of these epilayers, corresponding to a sample with $x = 0.42$ (sample A1018). As in the case of the PL measurements, the CL spectra are dominated by a single peak. The inset of the figure shows a mapping of the CL peak wavelength corresponding to a sample area of $2 \mu\text{m} \times 6 \mu\text{m}$. As can be seen in the figure, the CL signal is highly homogeneous, with peak-wavelength variations that are lower than 3 nm over the whole area investigated. Similar results were obtained in the rest of samples investigated with the exception of sample A1004 ($x = 0.33$), where small submicron domains weakly emitting 0.2–0.3 eV below the average emission energy were found to appear in the CL mappings. Such CL signal, arising from regions with slightly larger In contents, is fully compatible with the broadening of the HRXRD reflections and may be attributed to dot-like In-rich regions near the surface of the InGaN epilayers.^{31,32} In the rest of epilayers the CL signal was highly homogeneous, with no evidence of InN-rich segregated phases.

B. Raman scattering by $A_1(\text{LO})$ and E_{2h} phonons

Figure 3 shows Raman spectra of four representative $\text{In}_x\text{Ga}_{1-x}\text{N}$ epilayers. The measurements of Fig. 3 were excited at room temperature with 325.0-nm radiation. Although this excitation wavelength (3.81 eV) is far away from the fundamental band-gap of the $\text{In}_x\text{Ga}_{1-x}\text{N}$ samples investigated in this work (~ 2.4 eV for $x \sim 0.3$), a significant intensity enhancement of the $A_1(\text{LO})$ mode in relation to the E_{2h} peaks is observed with increasing Ga content. This indicates that the Fröhlich interaction mechanisms contribute strongly to the $A_1(\text{LO})$ signal observed in the Ga-rich samples. Taking into account the large energy difference between the excitation radiation and the fundamental band-gap of the samples, the enhancement of the $A_1(\text{LO})$ bands with increasing Ga content can be attributed to a disorder-induced broadening of the resonance profile. Similar results have been reported in disordered III-nitride samples such as ion-beam implanted GaN.³³

The spectra of Fig. 3 exhibit the expected one-mode behavior for both the E_{2h} and $A_1(\text{LO})$ modes, as predicted by the MREI model²⁵ and reported in previous studies over

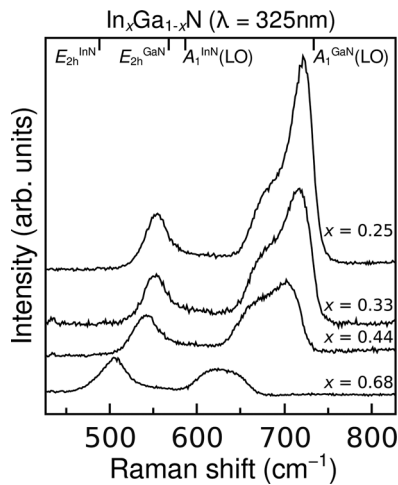


FIG. 3. Selected room-temperature Raman spectra of the $\text{In}_x\text{Ga}_{1-x}\text{N}$ epilayers studied in this work, excited with 325.0-nm radiation. The marks on the top axis show the frequency position of the E_{2h} and $A_1(\text{LO})$ modes of the pure binary end members of the alloy. For scaling reasons, the spectra have been normalized to the E_{2h} intensity and vertically shifted.

the entire composition range of the alloy.^{15,16} A broad feature is also visible in all the spectra below the $A_1(\text{LO})$ band.^{12,13,15,17,19} The intensity of this band, which is usually labeled as “S band” in the literature,^{12,17} is maximum in relation to the E_{2h} mode for intermediate In compositions, i.e., in the samples with the highest degree of alloy disorder. Thus, most authors attribute this feature to Raman scattering by disorder-activated optical modes arising from alloy disorder. As discussed in Ref. 17, it cannot be ruled out that this band has an important contribution from the B_1 silent mode.

When the laser excitation approaches the direct bandgap of $\text{In}_x\text{Ga}_{1-x}\text{N}$, the $A_1(\text{LO})$ band displays a dramatic intensity increase because the $A_1(\text{LO})$ phonon is resonantly excited via the Fröhlich interaction mechanisms. This is illustrated in Fig. 4, which shows selected room-temperature Raman spectra of the InGaN epilayers studied in this work, excited with the 514.5-nm line of an Ar^+ laser. This excitation wavelength yields resonant or near resonant conditions for the Ga-rich samples. In this case, strong multiphonon bands are also observed (not shown, see for instance Refs. 15 and 16). In the particular case of the sample with

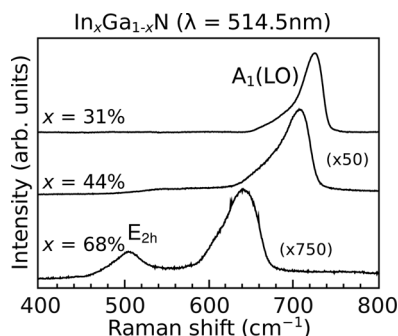


FIG. 4. Selected room-temperature Raman spectra of the $\text{In}_x\text{Ga}_{1-x}\text{N}$ epilayers studied in this work, excited with 514.5-nm light. The spectra have been normalized and vertically shifted for scaling reasons. In the spectra of the Ga-rich epilayers, a strong luminescence background has also been subtracted.

$x = 0.68$, the bandgap of which is lower than 1.3 eV, the 514.5-nm spectrum (Fig. 4) shows an increased $A_1(\text{LO})/E_{2h}$ intensity ratio in relation to the 325.0-nm spectrum (Fig. 3). Thus, in the 514.5-nm spectra of the In-rich samples the Fröhlich mechanisms still contribute to the $A_1(\text{LO})$ signal, which again is a consequence of disorder-induced broadening of the resonance profile.

Figure 5 shows the composition dependence of the $A_1(\text{LO})$ peak frequency for all the samples studied in this work as obtained from the 325.0- and 514.5-nm Raman spectra. In the case of the two In-rich samples it was not possible to determine the $A_1(\text{LO})$ peak frequency from the UV measurements because, as can be seen in Fig. 3, the $A_1(\text{LO})$ mode is weaker and superimposed to the S band. In Fig. 5 the solid line represents the frequency behavior predicted by the MREI model,²⁵ i.e., the linear interpolation between the GaN and InN frequency values. Even considering the relatively large errors associated with the In content determination by HRXRD, it is clear that the Ga-rich samples ($x < 0.5$) do not follow the frequency dependence predicted by the MREI model, while only the In-rich samples seem to exhibit the linear behavior. Similar observations were reported by Hernández *et al.*¹⁵ and by Ager *et al.*,¹⁶ who found that in the $0.2 < x < 0.5$ range the frequency of the $A_1(\text{LO})$ mode tends to be significantly upshifted in relation to the predictions of the MREI model. On the other hand, the figure also shows that the peak frequencies extracted from the visible spectra are consistently higher, around 7–10 cm^{-1} , than those obtained with the UV measurements. The possible origin of these shifts will be discussed later.

C. Strain-corrected $A_1(\text{LO})$ and E_{2h} frequencies

As observed by HRXRD, our Ga-rich samples exhibit significant degrees of lattice strain. On the other hand, the fact that only the In-rich (i.e., fully-relaxed) samples seem to follow the frequency behavior predicted by the MREI model suggests that the $A_1(\text{LO})$ frequency of the Ga-rich epilayers must be strongly affected by strain. To further evaluate this point, we have calculated the $A_1(\text{LO})$ frequency in strain-free $\text{In}_x\text{Ga}_{1-x}\text{N}$, $\omega_0(x)$, as a function of the In molar fraction (x) by using the $A_1(\text{LO})$ frequencies measured in our samples, ω_{exp} , and correcting them for strain according to the plastic

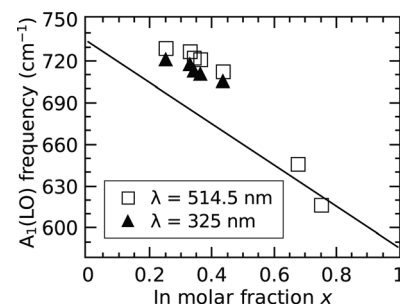


FIG. 5. Experimental frequency values for the $A_1(\text{LO})$ mode of InGaN as a function of In composition. Squares correspond to visible measurements (514.5-nm excitation) whereas triangles correspond to UV experiments (325 nm). The solid line displays the composition dependence of the $A_1(\text{LO})$ frequency predicted by the modified random-element isodisplacement model (Ref. 25).

relaxation values obtained by HRXRD (see Table I). Note that in the case of the two In-rich epilayers, the strain-corrected frequency values just correspond to the experimental frequencies, since these two samples are fully relaxed as indicated by the HRXRD measurements. For the calculations, we have assumed biaxial strain conditions and we have used the standard expression for the strain-induced phonon frequency shift in wurtzite compounds together with the appropriate phonon deformation potentials, $a_\lambda(x)$ and $b_\lambda(x)$, as a function of In content,

$$\omega_0(x) = \omega_{\text{exp.}} - \left(b_\lambda(x) - \frac{a_\lambda(x)C_{33}(x)}{C_{13}(x)} \right) \epsilon_\perp, \quad (1)$$

where $C_{13}(x)$ and $C_{33}(x)$ are elastic constants for the wurtzite crystal and $\epsilon_\perp = [(c - c_0)/c_0]$ is the out-of-plane component of the biaxial strain, with $c_0 = xC_{\text{InN}} + (1 - x)C_{\text{GaN}}$. The phonon deformation potentials for the pure GaN and InN compounds have been taken from Refs. 34 and 35, and we have used the $A_1(\text{LO})$ frequency values obtained with the non-resonance measurements (325.0 nm in the case of the Ga-rich samples) to minimize possible frequency shifts arising from selective resonant-excitation effects (see discussion below). We show in Fig. 6 the resulting frequency values for the $A_1(\text{LO})$ mode in strain-free $\text{In}_x\text{Ga}_{1-x}\text{N}$ as a function of x . As can be seen in the figure, the strain-corrected $A_1(\text{LO})$ frequencies are much closer to those predicted by the MREI model, which confirms that strain strongly affects the frequency behavior of the $A_1(\text{LO})$ mode of the InGaN alloy. Similar conclusions were reached by Correia *et al.*¹² on pseudomorphic $\text{In}_x\text{Ga}_{1-x}\text{N}$ epilayers in the low-In composition range ($x < 0.11$). In that work, the $A_1(\text{LO})$ mode was found to be almost composition independent owing to the opposite contribution of biaxial strain and In content. In the case of the present work, the observed deviations between calculated and experimental $A_1(\text{LO})$ frequencies (Fig. 6) can be most probably attributed to the relatively large errors in the evaluation of the strain and composition of the samples by HRXRD, and also to errors in the phonon deformation potential values used in the calculations. However, as can be seen in Fig. 6, the strain-corrected $A_1(\text{LO})$ frequency values are still higher than the predictions of the MREI model. With regard to this, one should also recall that the probe depth of the UV Raman measurements (a few nanometers) is much

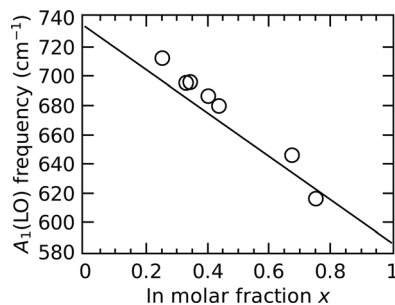


FIG. 6. Strain-corrected frequency of the $A_1(\text{LO})$ mode of the $\text{In}_x\text{Ga}_{1-x}\text{N}$ epilayers studied in this work as a function of x . The solid line represents the linear composition dependence predicted by the modified random-element isodisplacement model (Ref. 25).

smaller than that of the HRXRD measurements. Thus, the effective R values corresponding to the shallowest regions of the epilayers probed by the UV light (i.e., the more relaxed regions) may be expected to be larger than the R values given in Table I. This implies that the $A_1(\text{LO})$ frequency values of Fig. 6 have been overcorrected (i.e., the strain-corrected $A_1(\text{LO})$ frequency values of the figure should actually lie more separated from the MREI predictions). More work should be carried out in order to ascertain if the results of Fig. 6 can be solely attributed to experimental errors or to an additional effect. For instance, the observed deviations could be originated by a contribution of the forbidden $E_1(\text{LO})$ mode due to disorder or to sample mosaicity, as occurs in disordered III-nitrides^{36,37} or in nanostructured material.^{38,39}

A similar analysis using the appropriate phonon deformation potentials can be applied to obtain the compositional dependence of the frequency of the E_{2h} mode in strain-free $\text{In}_x\text{Ga}_{1-x}\text{N}$. Figure 7 shows the calculated frequency values for the E_{2h} mode of strain-free $\text{In}_x\text{Ga}_{1-x}\text{N}$ for the samples studied in this work. a_λ and b_λ values for the E_{2h} mode of GaN and InN have been taken from Refs. 34 and 35. For the In-rich samples the E_{2h} data points just correspond to the experimental values since, as observed by HRXRD, these samples are fully relaxed. In the figure, we have included data points from Refs. 10 and 21 and also from the In-rich samples of Ref. 16. Clearly, the strain-corrected E_{2h} frequencies do not follow the expected linear dependence predicted by the MREI model²⁵ but exhibit a marked bowing effect. A fit to the data of Fig. 7 with an expression of the type $\omega(x) = x\omega_{\text{InN}} + (1 - x)\omega_{\text{GaN}} - bx(1 - x)$, where $\omega(x)$ is the frequency of the E_{2h} mode for a given composition x , yields a value of $b = 46 \text{ cm}^{-1}$. In Ref. 10, a similar observation in $\text{In}_x\text{Ga}_{1-x}\text{N}$ films with $x < 0.5$ led the authors to conclude that the E_{2h} mode exhibits a two-mode behavior, as occurs in $\text{Al}_x\text{Ga}_{1-x}\text{N}$.⁴⁰ In the present work, using data over the whole composition range, we conclude that the E_{2h} mode of $\text{In}_x\text{Ga}_{1-x}\text{N}$ exhibits a one-mode behavior and suffers a strong bowing effect. Very recent work by Kim *et al.*²¹ seems to point in the same direction. The observed frequency bowing might be related to a disorder-induced mixing between the E_{2h} and $E_1(\text{TO})$ phonons, since the atomic vibrations of these

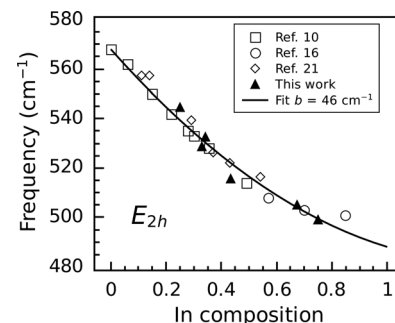


FIG. 7. Strain-corrected E_{2h} frequency values vs In molar fraction for the InGaN epilayers studied in this work (triangles). Additional data reported in the literature from strain-free samples have been included in the plot (squares and circles). The solid line shows the result of a parabolic fit for all the experimental points. From the fit, a bowing parameter equal to 46 cm^{-1} was obtained.

two modes are both perpendicular to the c axis of wurtzite. In the case of $\text{Al}_x\text{Ga}_{1-x}\text{N}$, it has been reported that the E_{2h} and $E_1(\text{TO})$ peaks from different scattering configurations have identical shapes and frequencies, which has been attributed to mixing of these two modes.⁴⁰ More work is necessary in order to fully understand the origin of these observations.

D. Dependence on the excitation wavelength of the $A_1(\text{LO})$ frequency

As observed in Fig. 5, the $A_1(\text{LO})$ peak frequencies obtained from the UV Raman spectra of our $\text{In}_x\text{Ga}_{1-x}\text{N}$ samples ($0.25 < x < 0.45$) are consistently lower than those obtained with the visible measurements. Note that the present measurements did not allow us to study the wavelength dependence of the E_{2h} peaks, since this mode was only visible under non-resonant excitation conditions.

Significant frequency variations of the $A_1(\text{LO})$ mode of InGaN as a function of the excitation wavelength have been reported in the literature.^{13,15,17–19} Different effects such as strain/compositional gradients,^{13,19} selective resonant excitation,^{5,7,15,17} or disorder-induced breakdown of wave-vector conservation¹⁸ have been invoked to explain the observed shifts.

With regard to the latter effect, it should be noted that the participation of phonons with increased wave-vectors for excitation wavelengths approaching the band-gap of the material would be expected to yield lower $A_1(\text{LO})$ frequencies.¹⁸ In the case the present study we observe the opposite effect, i.e., close to resonance (514.5 nm) the frequency of the $A_1(\text{LO})$ mode in the Ga-rich samples is significantly higher than in the case of the UV spectra. Hence, wave-vector non-conservation can be ruled out as the underlying mechanism giving rise to the results of Fig. 5.

On the other hand, strain and/or compositional gradients are good candidates to explain the observed frequency variations of the $A_1(\text{LO})$ mode.^{13,19} The presence of in-depth strain and composition gradients in the InGaN alloy seems to depend on the particular growth method and growth conditions. For instance, Pereira *et al.*²⁹ showed that the relaxation of strain in InGaN epilayers grown by metal organic chemical vapor deposition (MOCVD) is accompanied by increased In contents. Similarly, Wang *et al.*⁴¹ reported increased In contents along the growth direction in Ga-rich InGaN layers grown by MOCVD. Quantum-dot-like emission from In-rich regions arising from the upper part of MOCVD-grown InGaN epilayers has been reported.³² On the other hand, the laterally averaged In content was found to be constant, and even to slightly decrease along the growth direction, in InGaN epilayers grown by MBE.⁴²

Bearing in mind the strong impact of strain on the frequency of the $A_1(\text{LO})$ and E_{2h} phonons of InGaN (see Fig. 6 and related discussion), one should recall that the 325.0-nm excitation radiation only probes the shallowest regions of the epilayers (~ 35 nm in the case of GaN). Thus, the lower $A_1(\text{LO})$ peak frequency obtained with the UV Raman measurements in the Ga-rich samples might be partly accounted for by a higher degree of strain relaxation and/or a higher In content of the shallowest regions in comparison to the deeper

regions probed by the 514.5-nm light. As discussed in Sec. III A, the x-ray reflections observed with HRXRD are fairly broad, indicating that strain and/or composition gradients may exist in the epilayers along the growth direction. Unfortunately, given that the enhancement of In content along the growth direction is in general linked to the strain relaxation of the InGaN films,⁴¹ it is very difficult to discriminate between in-depth strain gradients and composition gradients from the Raman spectra alone.

To understand the results of Fig. 5 and also to shed additional light on the origin of the large dispersion of results in the literature regarding the behavior of the $A_1(\text{LO})$ mode of $\text{In}_x\text{Ga}_{1-x}\text{N}$, we have performed a series of simple calculations to evaluate the impact of lateral compositional fluctuations and of strain/composition gradients on the frequency of this mode. The aim of such calculations is not to find out the exact mechanism underlying our experimental results and those reported in the literature, but to provide additional clues about the impact of each effect on the Raman spectra of InGaN alloys.

1. In-depth composition and strain gradients under non-resonant conditions

First, we concentrate on in-depth composition gradients for non-resonance Raman scattering by the $A_1(\text{LO})$ mode of InGaN. We make use of the Δc value extracted from the HRXRD spectra and assume, for simplicity, that all the broadening of the (00.2) x-ray reflections (see Fig. 1) solely arises from in-depth compositional gradients, with no contribution of strain gradients. As discussed in Sec. III A, we estimate that the observed peak broadening roughly corresponds to lattice-parameter variations lower than 0.03 Å. Using Vegard's law for the composition dependence of the relaxed lattice parameter of $\text{In}_x\text{Ga}_{1-x}\text{N}$, we infer that the maximum in-depth composition gradients that may be present in our samples are of the order of $\Delta x = 0.05\text{--}0.08$. Taking into account the linear composition dependence of the $A_1(\text{LO})$ mode of InGaN predicted by the MREI model, we estimate that such x variations should yield frequency shifts of about $7\text{--}12\text{ cm}^{-1}$, consistent with the frequency shift of the $A_1(\text{LO})$ mode that we observe between the visible and UV Raman measurements ($7\text{--}10\text{ cm}^{-1}$).

Conversely, if we assume that all the broadening observed by HRXRD in the (00.2) reflections is solely originated by in-depth strain gradients, the corresponding $A_1(\text{LO})$ frequency variation can be estimated through error propagation arguments from the derivative of Eq. (1) and employing the definition of ϵ_{\perp} ,

$$\Delta\omega_{\text{exp}} = \left(b_{\lambda}(x) - \frac{a_{\lambda}(x)C_{33}(x)}{C_{13}(x)} \right) \frac{\Delta c}{c_0(x)}. \quad (2)$$

By using this expression together with the value $\Delta c \lesssim 0.03\text{ Å}$ extracted from the x-ray reflections, we estimate that the $A_1(\text{LO})$ mode of $\text{In}_x\text{Ga}_{1-x}\text{N}$ should exhibit frequency shifts of $\sim 10\text{--}12\text{ cm}^{-1}$ in our samples. These values are also compatible with the observed frequency shift exhibited by the $A_1(\text{LO})$ mode observed in our samples as a function of the

excitation wavelength. Following these analyses, it can be concluded that a combination of in-depth strain relaxation and compositional gradients may be very well responsible for the consistently higher $A_1(\text{LO})$ frequency values measured in our samples with 514.5-nm radiation relative to the 325.0-nm spectra.

2. Selective resonance excitation

The previous discussion has been restricted to non-resonant conditions. Lateral compositional fluctuations have not been considered since they are expected to yield broadening of the Raman peaks, with no effect on the $A_1(\text{LO})$ frequency. With regard to resonant excitation, several authors have reported frequency shifts of the $A_1(\text{LO})$ mode of InGaN as a function of the excitation wavelength that are most likely related to selective resonant excitation of regions with different In contents.^{5,7,15,17} In general, however, it is not easy to discriminate in a particular sample between strain effects and the selective excitation of the $A_1(\text{LO})$ band, since both types of effects may yield frequency shifts of equal or opposite direction depending on the excitation wavelength used to perform the Raman experiments. Note also that the magnitude of the selective excitation on the frequency behavior of the $A_1(\text{LO})$ mode is expected to depend upon the particular degree of compositional inhomogeneity of the sample under study.

To qualitatively illustrate the effect of selective excitation on the frequency of the $A_1(\text{LO})$ frequency of $\text{In}_x\text{Ga}_{1-x}\text{N}$, we have performed a simple calculation of the $A_1(\text{LO})$ phonon frequency under resonant excitation for a sample in which the compositional inhomogeneity is assumed to follow a Gaussian distribution. For simplicity, we consider only lateral compositional fluctuations and neglect the effect of in-depth fluctuations, since these should yield modified $A_1(\text{LO})$ line shapes due to the depth dependence of the absorption coefficient related to different In contents. Within this crude approach, theoretical Raman line shapes may be obtained with the following expression:

$$I(\omega) = \int \exp\left(-\frac{(x' - x)^2}{2\sigma^2}\right) \mathcal{L}[\omega(x')] \frac{1}{[E_{\text{exc}} - E_g(x')]^2 + \Gamma_g^2} dx', \quad (3)$$

where the first term in the integral corresponds to a Gaussian distribution centered at a composition x and standard deviation equal to σ . In the previous expression, $\mathcal{L}(\omega)$ represents a Lorentzian function for the $A_1(\text{LO})$ bands arising from domains with an In content equal to x' (i.e., a Lorentzian function centered at a frequency $\omega(x') = x'\omega_{\text{InN}} + (1 - x')\omega_{\text{GaN}}$ as given by the MREI model). For simplicity, we have taken a constant full-width at half maximum for the Lorentzian function $\mathcal{L}[\omega(x')]$ equal to $\Gamma = 5 \text{ cm}^{-1}$. The last term of Eq. (3) represents the profile of the resonant enhancement for the Fröhlich interaction mechanisms which, following Ref. 43, we have taken as a Lorentzian function. In the last term of the equation, E_{exc} stands for the energy of the excitation radiation, $E_g(x')$ is the fundamental bandgap of the alloy for domains with a composition x' , and Γ_g is the broadening

parameter of the resonance profile. For simplicity, we have assumed that Γ_g does not depend on In content, and we have taken a value $\Gamma_g = 0.1 \text{ eV}$ to model the broad resonance profile of the InGaN alloy.¹⁶

Figure 8 shows $A_1(\text{LO})$ peak frequencies obtained with Eq. (3) as a function of the energy of E_{exc} , for $\text{In}_x\text{Ga}_{1-x}\text{N}$ material with an average In content of $x = 0.3$ and different σ values. As can be seen in the figure, for resonant excitation below the bandgap energy (2.32 eV for $x = 0.3$) Eq. (3) predicts a downward frequency shift of the $A_1(\text{LO})$ mode due to the compositional fluctuations, with a minimum $A_1(\text{LO})$ peak frequency value that depends on σ . As expected, the effect of the compositional inhomogeneity on the frequency shifts becomes larger when σ is increased. For lower E_{exc} values, far away from resonance, the theoretical $A_1(\text{LO})$ peak frequency tends to the $A_1(\text{LO})$ frequency corresponding to the average composition of the sample (x in Eq. (3)). Conversely, the lateral composition fluctuations give rise to an upward frequency shift of the $A_1(\text{LO})$ mode for above-bandgap excitation, reaching a maximum that again depends on σ . As can be seen in the figure, Eq. (3) predicts strong shifts of the $A_1(\text{LO})$ peak frequency, relative to the average $A_1(\text{LO})$ frequency, for excitation wavelengths just around the average bandgap value of the material. In particular, the model predicts frequency shifts as large as 10 cm^{-1} for $\sigma = 6\%$. Note that similar compositional fluctuations, and comparable upward frequency shifts for near-resonant above-bandgap excitation, have been reported in the literature and attributed to compositional fluctuations.⁷ Thus, leaving aside the simplicity of this model, the results of Fig. 8 show that selective resonance effects also play an important role in the behavior of the $A_1(\text{LO})$ mode in InGaN material with significant degrees of compositional inhomogeneity. This is clearly the case of many of the samples studied in the literature.^{5,7,15,17}

With regard to the samples studied in this work, the higher $A_1(\text{LO})$ frequencies measured in the Ga-rich epilayers ($0.25 < x < 0.45$) under near-resonant excitation (514.5 nm) in relation to the UV spectra (see Fig. 5) might be partly explained by selective resonant-excitation effects. However,

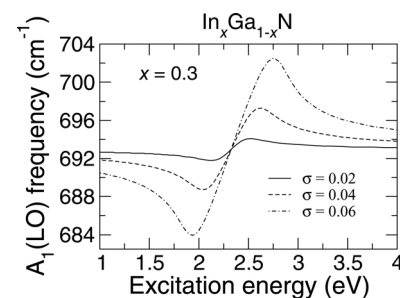


FIG. 8. Calculated $A_1(\text{LO})$ frequency of $\text{In}_x\text{Ga}_{1-x}\text{N}$ for resonant Raman-scattering measurements as a function of the excitation energy. The theoretical curves are obtained within a simple approach in which the effect of selective resonant excitation due to lateral compositional fluctuations is evaluated by assuming that the compositional inhomogeneities follow a Gaussian distribution centered at a composition x . σ is the standard deviation of the Gaussian distribution. The curves in the figure were obtained for $x = 0.3$ and different values of σ .

as can be seen in Fig. 5, all the $A_1(\text{LO})$ frequency values extracted from the 514.5-nm spectra exhibit comparable frequency shifts relative to the UV data, ranging from 7 up to $\sim 10 \text{ cm}^{-1}$. In contrast, the corresponding bandgap values of these samples is drastically reduced from $\sim 2.3 \text{ eV}$ for $x = 0.25$ down to $\sim 1.6 \text{ eV}$ for $x = 0.43$. Thus, different frequency shifts arising from selective resonance effects should be expected for these samples. The almost constant frequency shift observed between the UV and visible spectra, together with the high lateral homogeneity of the epilayers as observed by CL (see Sec. III A), suggests that in-depth strain/composition gradients are probably the main factors responsible for the wavelength dependence of the $A_1(\text{LO})$ frequency in the samples studied in this work.

IV. CONCLUSION

We have performed Raman-scattering measurements on a series of $\text{In}_x\text{Ga}_{1-x}\text{N}$ epilayers grown by MBE with In contents in the 0.25-0.75 range. The Raman spectra of Ga-rich samples ($0.25 < x < 0.44$) reveal that the frequency of the $A_1(\text{LO})$ mode is significantly higher than that calculated within the framework of the MREI model,²⁵ which predicts a linear composition dependence between the GaN and InN $A_1(\text{LO})$ frequencies. In the case of In-rich samples, which are fully relaxed, the experimental $A_1(\text{LO})$ frequencies are in much better agreement with the predictions of the MREI model. The deviations observed for $0.25 < x < 0.44$ can be accounted for if the strain state of the layers is taken into account. We have performed HRXRD measurements to evaluate the In content and strain relaxation of the samples, and we have shown that the strain-corrected $A_1(\text{LO})$ frequency values are in agreement with the MREI model. We have analyzed the effect of in-depth strain gradients, in-depth composition gradients and selective resonant excitation on the frequency of the $A_1(\text{LO})$ mode of $\text{In}_x\text{Ga}_{1-x}\text{N}$. These effects have a strong impact on the frequency of this mode, making very difficult to evaluate the strain state and/or the composition of the InGaN material from the $A_1(\text{LO})$ peak frequency alone. In the case of the E_{2h} mode, we have shown that the strain-corrected frequencies exhibit a clear bowing effect over the whole composition range in relation to the linearly interpolated values predicted by the MREI model. This bowing effect has to be taken into account to evaluate from the E_{2h} frequency the composition and/or the strain state of InGaN material.

ACKNOWLEDGMENTS

Work supported by the Spanish Ministry of Science and Innovation (MICINN) through Project MAT2010-16116.

¹W. Walukiewicz, J. W. Ager III, K. M. Yu, Z. Liliental-Weber, J. Wu, S. X. Li, R. E. Jones, and J. D. Denlinger, *J. Phys. D: Appl. Phys.* **39**, R83 (2006).

²J. Wu, *J. Appl. Phys.* **106**, 011101 (2009).

³J. Menéndez, *Raman Scattering in Materials Science*, Springer Series in Materials Science, edited by W. H. Weber and R. Merlin (Springer-Verlag, Berlin Heidelberg, 2000), Chap. 3, Vol. 42.

⁴H. Harima, *J. Phys.: Condens. Matter* **14**, R967 (2002).

- ⁵D. Behr, J. Wagner, A. Ramakrishnan, H. Obloh, and K. H. Bachem, *Appl. Phys. Lett.* **73**, 241 (1998).
- ⁶H. Harima, E. Kurimoto, Y. Sone, S. Nakashima, S. Chu, A. Ishida, and H. Fujiyasu, *Phys. Stat. Sol. (b)* **216**, 785 (1999).
- ⁷N. Wieser, O. Ambacher, H. P. Felsl, L. Görgens, and M. Stutzmann, *Appl. Phys. Lett.* **74**, 3981 (1999).
- ⁸A. Kaschner, A. Hoffmann, C. Thomsen, T. Böttcher, S. Einfeldt, and D. Hommel, *Phys. Stat. Sol. (a)* **179**, R4 (2000).
- ⁹T. Sugiura, Y. Kawaguchi, T. Tsukamoto, H. Andoh, M. Yamaguchi, K. Hiramatsu, and N. Sawaki, *Jpn. J. Appl. Phys.* **40**, 5955 (2001).
- ¹⁰D. Alexson, L. Bergman, R. J. Nemanich, M. Dutta, M. A. Stroschio, C. A. Parker, S. M. Bedair, N.A. El-Masry, and F. Adar, *J. Appl. Phys.* **89**, 798 (2001).
- ¹¹V. Yu. Davydov, A. A. Klochikhin, V. V. Emtsev, A. N. Smirnov, I. N. Goncharuk, A. V. Sakharov, D. A. Kurdyukov, M. V. Baidakova, V. A. Vekshin, S. V. Ivanov, J. Aderhold, J. Graul, A. Hashimoto, and A. Yamamoto, *Phys. Stat. Sol. (b)* **240**, 425 (2003).
- ¹²M. R. Correia, S. Pereira, E. Pereira, J. Frandon, and E. Alves, *Appl. Phys. Lett.* **83**, 4761 (2003).
- ¹³M. R. Correia, S. Pereira, E. Pereira, J. Frandon, I. M. Watson, C. Liu, E. Alves, A. D. Sequeira, and N. Franco, *Appl. Phys. Lett.* **85**, 2235 (2004).
- ¹⁴M. Bosi, R. Fornari, S. Scardova, M. Avella, O. Martinez, and J. Jiménez, *Semicond. Sci. Technol.* **19**, 147 (2004).
- ¹⁵S. Hernández, R. Cuscó, D. Pastor, L. Artús, K. P. O'Donnell, R. W. Martin, I. M. Watson, Y. Nanishi, and E. Calleja, *J. Appl. Phys.* **98**, 013511 (2005).
- ¹⁶J. W. Ager III, W. Walukiewicz, W. Shan, K. M. Yu, S. X. Li, E. E. Haller, H. Lu, and W. J. Schaff, *Phys. Rev. B* **72**, 155204 (2005).
- ¹⁷A. G. Kontos, Y. S. Raptis, N. T. Pelekanos, A. Georgakilas, E. Bellet-Amalric, and D. Jalabert, *Phys. Rev. B* **72**, 155336 (2005).
- ¹⁸V. Y. Davydov, A. A. Klochikhin, I. N. Goncharuk, A. N. Smirnov, A. V. Sakharov, A. P. Skvortsov, M. A. Yagovkina, V. M. Lebedev, H. Lu, and W. J. Schaff, *Phys. Stat. Sol. (b)* **243**, 1494 (2006).
- ¹⁹A. Kar, D. Alexson, M. Dutta, and M. Stroschio, *J. Appl. Phys.* **104**, 073502 (2008).
- ²⁰E. Tiras, M. Gunes, N. Balkan, and W. J. Schaff, *Phys. Status Solidi B* **247**, 189 (2010).
- ²¹J. G. Kim, Y. Kamei, A. Kimura, N. Hasuike, H. Harima, K. Kisoda, T. Hotta, K. Sasamoto, and A. Yamamoto, *Phys. Status Solidi C*, "Observation of $A_1(\text{LO})$, $E_2(\text{high})$ and $B_1(\text{high})$ phonon modes in $\text{In}_x\text{Ga}_{1-x}\text{N}$ alloys with $x = 0.11-0.54$," (in press). DOI 10.1002/pssc.201100401.
- ²²J. Wagner, A. Ramakrishnan, H. Obloh, and M. Maier, *Appl. Phys. Lett.* **74**, 3863 (1999).
- ²³S. Lazić, M. Moreno, J. M. Calleja, A. Trampert, K. H. Ploog, F. B. Naranjo, S. Fernandez, and E. Calleja, *Appl. Phys. Lett.* **86**, 061905 (2005).
- ²⁴H. C. Yang, P. F. Kuo, T. Y. Lin, Y. F. Chen, K. H. Chen, L. C. Chen, J. I. Chyi, *Appl. Phys. Lett.* **76**, 3712 (2000).
- ²⁵H. Grille, C. Schnittler, and F. Bechstedt, *Phys. Rev. B* **61**, 6091 (2000).
- ²⁶P. Misra, C. Boney, N. Medelci, D. Starikov, A. Freundlich, and A. Bensaoula, 33rd IEEE Photovoltaic Specialists Conference **1-4**, 1380 (2008).
- ²⁷R. Kudrawiec, M. Siekacz, M. Kryško, G. Cywiński, J. Misiewicz, and C. Skierbiszewski, *J. Appl. Phys.* **106**, 113517 (2009).
- ²⁸D. Holec, P. Costa, M. J. Kappers, and C. J. Humphreys, *J. Cryst. Growth* **303**, 314 (2007).
- ²⁹S. Pereira, M. R. Correia, E. Pereira, K. P. O'Donnell, E. Alves, A. D. Sequeira, N. Franco, I. M. Watson, and C. J. Deatcher, *Appl. Phys. Lett.* **80**, 3913 (2002).
- ³⁰G. Franssen, I. Gorczyca, T. Suski, A. Kamińska, J. Pereiro, E. Muñoz, E. Iliopoulos, A. Georgakilas, S. B. Che, Y. Ishitani, A. Yoshikawa, N. E. Christensen, and A. Svane, *J. Appl. Phys.* **103**, 033514 (2008).
- ³¹S. Srinivasan, F. Bertram, A. Bell, F. A. Ponce, S. Tanaka, H. Omiya, and Y. Nakagawa, *Appl. Phys. Lett.* **80**, 550 (2002).
- ³²Y. T. Moon, D. J. Kim, J. S. Park, J. T. Oh, J. M. Lee, Y. W. Ok, H. Kim, and S. J. Park, *Appl. Phys. Lett.* **79**, 599 (2001).
- ³³D. Pastor, J. Ibáñez, R. Cuscó, L. Artús, G. González-Díaz, and E. Calleja, *Semicond. Sci. Technol.* **22**, 70 (2007).
- ³⁴J. M. Wagner and F. Bechstedt, *Appl. Phys. Lett.* **77**, 346 (2000).
- ³⁵X. Q. Wang, S. B. Che, Y. Ishitani, and A. Yoshikawa, *Appl. Phys. Lett.* **89**, 171907 (2006).
- ³⁶R. Cuscó, J. Ibáñez, E. Alarcón-Lladó, L. Artús, T. Yamaguchi, and Y. Nanishi, *Phys. Rev. B* **79**, 155210 (2009).
- ³⁷J. Ibáñez, F. J. Manjón, A. Segura, R. Oliva, R. Cuscó, R. Vilaplana, T. Yamaguchi, Y. Nanishi, and L. Artús, *Appl. Phys. Lett.* **99**, 011908 (2011).

- ³⁸E. Alarcón-Lladó, J. Ibáñez, R. Cuscó, L. Artús, J. D. Prades, S. Estradé, and J. R. Morante, *J. Raman Spectr.* **42**, 153 (2011).
- ³⁹R. Cuscó, N. Domènech-Amador, L. Artús, T. Gotschke, K. Jeganathan, T. Stoica, and R. Calarco, *Appl. Phys. Lett.* **97**, 221906 (2010).
- ⁴⁰V. Y. Davydov, I. N. Goncharuk, A. N. Smirnov, A. E. Nikolaev, W. V. Lundin, A. S. Usikov, A. A. Klochikhin, J. Aderhold, J. Graul, O. Semchinova, and H. Harima, *Phys. Rev. B* **65**, 125203 (2002).
- ⁴¹H. Wang, D. S. Jiang, U. Jahn, J. J. Zhu, D. G. Zhao, Z. S. Liu, S. M. Zhang, and H. Yang, *Thin Solid Films* **518**, 5028 (2010).
- ⁴²H. Selke, M. Amirsawadkouhi, P. L. Ryder, T. Böttcher, S. Einfeldt, D. Hommel, F. Bertram, and J. Christen, *Mat. Sci. Eng. B* **59**, 279 (1999).
- ⁴³M. Cardona, in *Light Scattering in Solids II*, edited by M. Cardona and G. Güntherodt, Topics in Applied Physics Vol. 50 (Springer-Verlag, Berlin, 1982).